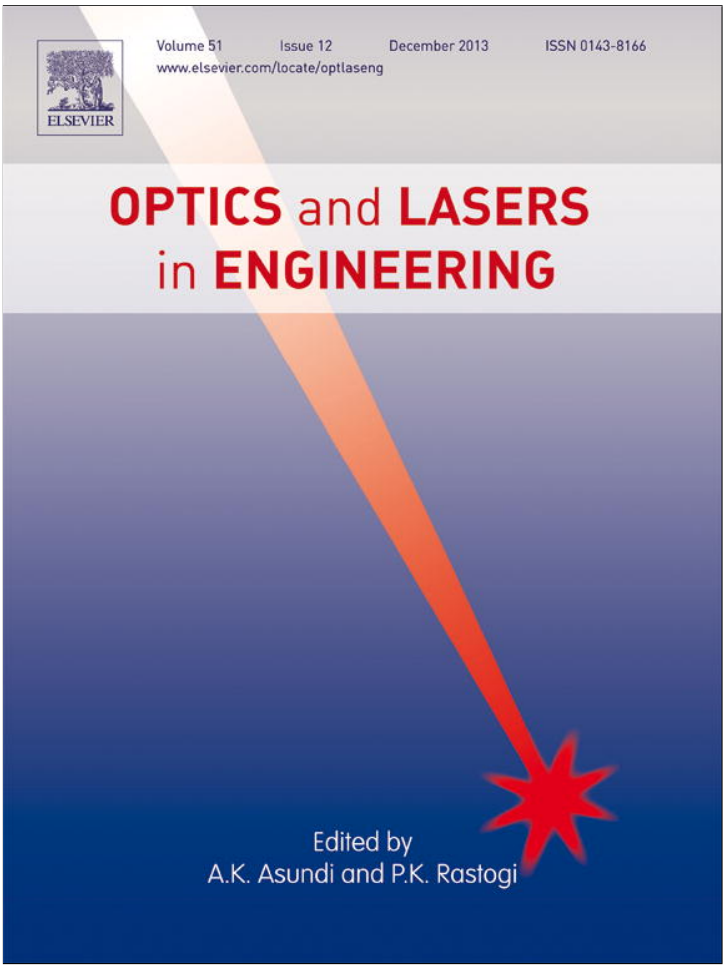

Optics and Lasers in Engineering 51 (2013) 1368–1378

Contents lists available at SciVerse ScienceDirect

Optics and Lasers in Engineering

journal homepage: www.elsevier.com/locate/optlaseng

Speckle pattern quality assessment for digital image correlation

G. Crammond, S.W. Boyd, J.M. Dulieu-Barton *

University of Southampton, Engineering Sciences, Southampton SO17 1BJ, UK

ARTICLE INFO

Article history:
Received 15 November 2012
Received in revised form
15 March 2013
Accepted 23 March 2013
Available online 27 June 2013

Keywords:
Speckle pattern quality
Morphological assessment
Digital image correlation (DIC)
High spatial resolution

ABSTRACT

To perform digital image correlation (DIC), each image is divided into groups of pixels known as subsets or interrogation cells. Larger interrogation cells allow greater strain precision but reduce the spatial resolution of the data field. As such the spatial resolution and measurement precision of DIC are limited by the resolution of the image. In the paper the relationship between the size and density of speckles within a pattern is presented, identifying that the physical properties of a pattern have a large influence on the measurement precision which can be obtained. These physical properties are often overlooked by pattern assessment criteria which focus on the global image information content. To address this, a robust morphological methodology using edge detection is devised to evaluate the physical properties of different speckle patterns with image resolutions from 23 to 705 pixels/mm. Trends predicted from the pattern property analysis are assessed against simulated deformations identifying how small changes to the application method can result in large changes in measurement precision. An example of the methodology is included to demonstrate that the pattern properties derived from the analysis can be used to indicate pattern quality and hence minimise DIC measurement errors. Experiments are described that were conducted to validate the findings of morphological assessment and the error analysis.

1. Introduction

Digital image correlation is a white light technique based on the comparison of images before, during and after the deformation of a test specimen, typically acquired using a monochromatic CCD camera. The images are divided into a grid of interrogation cells or subsets containing a finite number of pixels. The spatial resolution and accuracy of the displacements are limited by the total number of pixels within the image. DIC uses a correlation algorithm to obtain the displacements by identifying areas of matching grey scale values between the speckle pattern in each subset of the deformed and undeformed images. The position where the correlation function value is maximised in the deformed image corresponds to the movement of the pattern during deformation. To facilitate the correlation a stochastic speckle pattern is applied to the specimen surface to provide random grey level variations, the quality of which is fundamental to the precision of the measured displacement data. Spatial resolution of the data is maximised by reducing the size of the subsets, but as the interrogation cell size decreases, the uncertainty in the strain measurement increases due to a reduction in the number of features to track within the subset [1].

The majority of research into the accuracy of the DIC technique has focused on the many different correlation algorithms and processing parameters, such as subset size [2], shape function selection [3] and methods of obtaining sub-pixel accuracy [4]. Less attention has been paid to the effect of the quality of the speckle pattern on the measurement accuracy of the DIC technique, particularly, differences due to changes in the spatial resolution of the image. It is also important for the speckle pattern to be matched to the expected displacement field to maximise measurement accuracy, as speckles can be both too large and too small for accurate measurement [5]. In references [6,7] patterns with a range of speckle sizes, applied using different methods were examined. Haddadi and Belhabib [6] identified that finer patterns with more speckles and more 'randomness' performed better in comparison to larger 'dotted' patterns in ridged body motion tests. Barranger et al. [7] noted the importance of matching the pattern to the expected deformation, with differences between pattern types becoming greater at larger levels of strain. The reasons behind the performance differences for the patterns were not assessed, nor were the suitability of the patterns tested for different applied strain levels, allowing only qualitative conclusions to be made which cannot be used to benchmark pattern quality.

A number of pattern assessment criteria have been presented in the literature, generating a range of different pattern quality measurement parameters. These parameters do not provide the definition of a perfect pattern to be used, as there is insufficient

* Corresponding author. Tel.: +44 2380596522.
E-mail address: janice@soton.ac.uk (J.M. Dulieu-Barton).

0143-8166/$ - see front matter © 2013 Elsevier Ltd. All rights reserved.
http://dx.doi.org/10.1016/j.optlaseng.2013.03.014

control in the application of the speckle pattern or imaging methods to consistently achieve the same quality of pattern from user to user. Rather the parameters are best used as comparative assessment tools to inform application methods and inform error analyses of DIC measurements. Broadly these metrics can be separated into global and local assessments. Measures such as the sum of squared subset intensity gradients [8] and mean intensity gradient [9] have both been developed directly from an understanding of the sum of squared differences correlation algorithm, measuring pattern quality locally at each pixel location. However these two parameters are presented as a summation and a mean of the image intensity gradients at each pixel location within the entire image. This approach provides global measures from local criteria. The summation and mean values are not considered to be appropriate as the speckle pattern is stochastic across the region of interest and unrepresentative of the pattern quality, as there is no indication of the variation in quality across the image. This is important as the values can be significantly biased by areas with anomalously high or low intensity gradient values. The mean subset fluctuation [10] and subset entropy [2] provide metrics which assess the difference between the grey level of each pixel within the image to the mean grey level value of each subset, and the grey level values of the eight surrounding pixels at each location. These metrics are also calculated locally within the subset, and then presented as a mean, global, value for the whole of the image, ignoring variation between subsets in the pattern.

Morphological approaches have been used to apply local analysis of pattern quality based upon the physical properties of the pattern, such as the size and frequency of the speckles within the pattern [5,11]. Typically this is undertaken using an image thresholding technique, converting all pixels with grey levels above/below a certain threshold value into black and white values to form a binary image of the pattern. The thresholding method is a fast and practical solution, but can fail to identify the true edge of shapes in patterns. Alexander et al. [12] noted that the size and shape of the generated binary speckles are highly dependent upon the chosen grey level threshold value, which can result in the edge of the speckles being poorly defined and not representative of the actual speckle size or shape. The threshold method also prevents the identification of discrete speckles below/above the threshold values, which is especially evident where there is a very broad grey level distribution, or where the edges of the speckles are very soft. These local measures are more adept at quantifying differences between patterns due to changes in the application method or pattern style i.e. black paint on white background and vice versa, both of which are important considerations for experiments with different materials and scales. Importantly, using these morphometric techniques, the local information from within the pattern is not lost or masked in the attempt to form a global parameter from what are highly variable and complex analysis problems. As a result the local, morphometric, pattern analysis approach is used in this paper. For completeness a summary of recently used global and local pattern assessment criteria is provided in Table 1.

The aim of the present paper is to identify the relationship between the size and density of the speckles locally within an interrogation cell. The relationship is used to show that the morphometric properties, such as size, shape and distribution of the speckles in the pattern are an important indicator of pattern quality. An image processing approach is developed to analyse the properties of a number of speckle patterns, showing fundamental changes to the pattern as magnification levels and spatial resolution are increased. In the present paper a case study is presented that uses the morphological analysis to identify the most suitable pattern application method when conducting 2D DIC at the mesoscopic scale using magnifying optics. Under high levels of magnification the appearance of the patterns changes significantly, resulting in very different patterns to those viewed with lower magnification. The errors in the DIC measurements at this high magnification level are shown to be large due to the sparseness of the patterns. The local analysis demonstrates large differences in the properties of the speckles within the pattern's grey level between application methods. It is shown that a change from a spray paint to an airbrush has a large beneficial effect on the overall measurement error. This is supported by simulations of pattern deformations and experimental validation against strain gauge readings, which provide excellent agreement with the predicted results from the morphological assessment.

Table 1
Review of recent pattern assessment criteria.

	Pattern assessment criteria	Global	Local	Pros	Cons
Sum of square of subset intensity gradients [8]	$SSSIG=\sum_{i=1}^{N}\sum_{j=1}^{N}[f_{x,y}(x_{ij})]^2$	X		Intensity gradients directly used in the sum of squared differences correlation procedure Provides a direct measure between the pattern and correlation process.	Total value for image does not show variability within the pattern SSSIG does not describe how or why patterns are different to each other—difficult to comparatively analyse application methods.
Mean intensity gradient [9]	$\delta_f=\frac{\sqrt{f_x(x_{ij})^2+f_y(x_{ij})^2}}{WH}$	X		Intensity gradients directly used in the sum of squared differences correlation procedure.	Mean value for image introduces bias as the calculation as it does not show variability within the pattern.
Mean subset fluctuation [10]	$\frac{S_f=\sum_{P\in F}\sum_{i=1}^{3}\sum_{j=1}^{3}\left\lvert a_{ij}-\overline{a}\right\rvert}{HV}$	X		Compares pixel grey level values to the mean grey level value of each subset. Provides a measure of contrast within the pattern.	Mean value for image does not show variability within the pattern. Bias towards patterns with very high contrast where $\lvert a_{ij}-\overline{a}\rvert$ is maximised. Cannot distinguish influence of speckle size i.e. one large speckle of size 50 pixels in the subset will yield same results as 10 speckles each with an area of 5 pixels distributed within the subset.
Subset entropy [2]	$\frac{\delta=\sum_{P\in S}\sum_{i=1}^{8}\left\lvert I_P-I_i\right\rvert}{2^p MN}$	X		Identifies differences between each pixel to its surrounding 8 pixels grey levels giving an indication of the fluctuation, or 'randomness' of the pattern.	Mean value for image does not show variability within the pattern.
Speckle radius distribution [11]	Image thresholding		X	Fast and easy to implement.	Speckle radius does not account for speckle shape which influences speckle size. Threshold method inaccurate.
Average speckle size [5]	Image thresholding		X	Fast and easy to implement.	Average speckle size does not show variability within pattern. Threshold method inaccurate.

Table 2
Shannon entropy values of patterns over a range of spatial resolutions.

Spatial resolution	23	37	142	296	705
Shannon image entropy	1.0777	1.6753	3.1947	1.5191	0.8917

Table 3
Speckle pattern properties.

Pattern type	Area of interest (mm × mm)	Spray paint	Airbrush	Background colour	Speckle colour
A	3.45 × 2.88		X	Black	White
B	3.45 × 2.88		X	White	Black
C	3.45 × 2.88	X		Black	White
D	3.45 × 2.88	X		White	Black

2. Correlation procedure and experimental equipment

In recent years DIC has become very popular and hence there are many commercial and in-house software available to perform DIC with differently optimised correlation functions and calculation methods, most recently summarised by Pan et al. [13]. The work in the present paper describes the creation of a generic methodology to assess the quality of stochastic speckle patterns and their relative influence on the measurement error. As there are large visible differences between the speckle patterns examined in this paper, the results are largely unaffected by small differences in correlation methods. It was decided that commercial software should be used, so for consistency the LaVision DaVis 7.4 correlation software was used in all the analyses. The DaVis software implements a cross correlation approach by using inverse Fourier transforms. For each subset in the image, an array of correlation values, C, are created between the reference I_1 and deformed I_2 subsets of size $n \times n$ pixels. The correlation value for each integer displacement between the subsets within a search area, measuring $2n \times 2n$ surrounding the original subset is calculated as follows:

$$C(dx,dy) = \sum_{x=0,y=0}^{x<n,y<n} I_1(x,y)I_2(x+dx,y+dy),\ -\frac{n}{2} < dx,dy < \frac{n}{2} \qquad (1)$$

To increase the speed of the calculations the correlation function algorithm is applied at each integer displacement using inverse fast Fourier transforms as follows:

$$I_1 I_2 = IFFT^{-1}[\overline{FFT(I_1)}FFT(I_2)] \qquad (2)$$

The correlation function is maximised when there is a good match between the intensities of the two subsets I_1 and I_2. Areas of poor pattern match have low correlation coefficients. The location of the greatest correlation function corresponds to the location of the deformed subset relative to the reference, from which the image deformation is established. The final sub-pixel displacement accuracy is obtained from the maximum position of a two dimensional Gaussian fitting parameter, which is applied to the array of correlation function values using a Levenberg–Marquardt algorithm. The strains are evaluated numerically using a central differences approach. The influence of different correlation algorithms and sub-pixel calculation schemes are not evaluated, as the results show clear trend between the patterns tested, with large differences in error values, which are greater than the errors expected from alternative correlation approaches. As such the pattern analysis and morphological conclusions identified in this paper are largely independent of the correlation settings, demonstrating that the quality of the pattern to be vital to the quality of the correlation.

A 5 Mp 12 bit monochromatic LaVision E-lite camera was used to capture the experimental images. A LED ring flash light was used to provide consistent lighting for the data collection. The grey level distribution of the images was maximised over the 12 bit dynamic range of the camera, whilst avoiding saturation of the image. This ensured that any measurement errors would be due to the physical changes to the pattern as opposed to a change in the reduction of the dynamic range of the image, which is known to have an influence on the accuracy of DIC measurements [7]. A Sigma 105 mm lens was used to capture the images analysed in Table 2, and a Canon MP-e65 macro lens was used to image the patterns presented in Table 3.

3. Evaluation of simulated speckle pattern variations

It is desirable to have a pattern with high levels of unique features and randomness to maximise the correlation function response when a match is found in each interrogation cell. This reduces the uncertainty in matching the pattern from image to image. Therefore the quality of the speckle pattern has a large influence on the correlation function values created for areas of similar patterns, and hence the accuracy of the calculated displacements. Within each interrogation cell though, there are a finite number of pixels to create the pattern. Due to this limiting value, a trade-off exists between the number and size of features and subsequently the number of possible unique pattern permutations that can be created. Here it is investigated if the accuracy of the DIC strain measurement obtained from correlating the speckle pattern between images is related to the relationship between the relative size of the speckles and their density in each interrogation cell, i.e. the relationship between the coverage and the uniqueness of the pattern that can be created within a given number of pixels.

Speckles of very small size are registered on only a small number of pixels on the camera sensor. This increases the similarity in shape and size of speckles in the pattern, reducing the uniqueness of the pattern. Additionally because of camera noise and grey level fluctuations, small speckles produce large variations in the identification of their size, shape and position relative to their original features, which is detrimental to the accuracy of the measurement. Increasing speckle size decreases the randomness of the pattern position as the speckles occupy more space in the finite interrogation cell. However, larger speckles have a greater number of shape permutations, creating more uniquely defined individual speckles within the pattern. Larger speckles also register across more pixels, so there is less relative fluctuation and uncertainty in the speckle shape and size resulting from noise from the camera. Therefore the trade-off between size, shape, and density heavily influence the degree of speckle uniqueness, and is an important and often overlooked factor to consider when assessing the quality of the speckle pattern.

There is, of course, a constraint on maximising the uniqueness of the pattern and this is the total number of pixels available in the interrogation cell. To investigate this constrained relationship between the available pixels within the images, the size of the speckles, and the number of speckles within each interrogation cell a pattern generation program was developed. The program generated a test matrix of 64 unique 12 bit patterns with differing combinations of speckle radii, from 2 to 9 pixels radius, and number of speckles present within each subset measuring 128×128 pixels within the image, from 4 to 18 speckles in intervals of 2. Each generated image was 1408×1408 pixels and contained 121 subsets. The generation program allows a degree of random variation of the radius of speckle around its circumference, replicating the characteristic random shape of each speckle in a real pattern. The program is such that the variation is linked to the speckle radius, so smaller speckles have less variation in shape, whilst larger speckles have more shape variation. Two examples

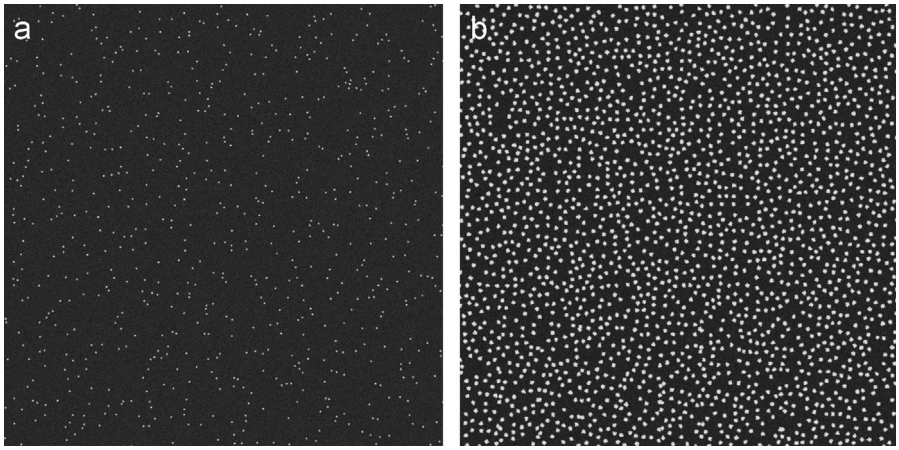

Fig. 1. (a) Generated pattern with six speckles per subset, and a speckle radius of 3 pixels. (b) Generated pattern with 18 speckles per subset, and a speckle radius of 8 pixels.

from the test matrix of 64 individually generated images can be seen in Fig. 1(a) and (b). The patterns were deformed in 0.1% intervals up to 2% maximum strain, with errors evaluated between the measured and calculated strain measurements using interrogation cell sizes of 128×128 pixels, with no overlap between subsets.

The x-direction displacements were derived by importing the speckle patterns into the LaVision correlation software DaVis 7.4. The location of the subsets analysed by the correlation software correspond to those defined in the pattern generation program, ensuring that each DIC interrogation cell has speckles of the same size and density. The pattern deformation was undertaken in the Fourier domain by upsampling the transform of the image then downsampling to achieve accurate sub-pixel displacements. A low pass filter was applied to the images before manipulation to remove high frequency components and minimise errors caused by image aliasing during the scaling process.

The images are deformed numerically so that errors from lighting and optical aberration effects are removed. Strains are obtained by numerical differentiation of the displacement vectors. Due to the uniform linear displacement field imposed on the image, minimal measurement errors are anticipated from this calculation approach. Errors are being assessed from the difference between the strain and not displacement data, as in engineering applications it is the strain data which is of most importance when analysing structures. It is important therefore to analyse the strain error so that an end user of DIC software can have confidence that the speckle pattern being used will result in high fidelity strain measurements. Large interrogation cells of 128×128 pixels are used in this study as the use of large interrogation cells produces measurements with a high degree of fidelity [1]. As a result, when using these large subsets, any differences in the strain derived from the DIC can be attributed to changes in the pattern properties, and not uncertainties resulting from poor quality correlation due to insufficient features in the interrogation cell. Gaussian noise was added to the deformed images to best replicate the experimental variation in pattern intensity due to noise from the camera CCD.

The standard deviation, SD, between the imposed strain field, $\varepsilon_{imposed}$, and the strain field derived from the DIC measurements, ε_{DIC}, in the x-direction was calculated for all of the measurement points, n, to give a value of the error due to the speckle pattern properties using the following equation:

$$SD_{\varepsilon} = \sqrt{\frac{n\sum(\varepsilon_{DIC}-\varepsilon_{imposed})^2-\left(\sum(\varepsilon_{DIC}-\varepsilon_{imposed})\right)^2}{n(n-1)}} \quad (3)$$

Fig. 2(a) and (b) shows an array of the mean error in the strain measurements from each of the 121 interrogation cells calculated within each of the 64 different generated images tested at 1% and 2% strain respectively. A clear gradient of error across both plots is visible, primarily running from left to right. This gradient shows greater mean measurement errors when there are fewer speckles per subset within the image. The error reduces when there are more speckles and a greater number of features in the pattern to track (i.e. from left to right in the plots the error reduces). A secondary gradient can also observed diagonally from bottom left to top right of the figures. This diagonal gradient indicates that for the same number of speckles per subset, patterns with larger speckles appear to produce a lower amount of error within the measurement, compared to patterns with smaller radius speckles. Hence increasing the size of the speckle, has an impact on the quality of the speckle pattern because the larger speckles have a greater variation in shape, creating very unique patterns. Fig. 2(a) and (b) also shows that the pattern is not improved by simply increasing the number of smaller speckles within the pattern to produce more features to track, and that there are a number of factors affecting pattern quality which must be considered.

Examination of the correlation function provides more explanation of the error trends. Fig. 3 shows a 2D view of the correlation function in a typical interrogation cell with 8 speckles per subset and a speckle radius of (a) 3 pixels, (b) 8 pixels. It can be seen in Fig. 3(a) that patterns with smaller radius speckles the correlation peak is very small, creating a very concentrated area where the pattern matches. Patterns with larger radii, Fig. 3(b) has a larger diameter to the footprint of the correlation function peak compared to the correlation peak, due to the increased coverage and shape definition of the pattern. The large footprint of the correlation peak in Fig. 3(b) is defined by a greater number of points than Fig. 3(a) so that the sub-pixel accuracy is increased because the Gaussian distribution used to define the correlation peak has more points, producing a better fit. When the speckle size is small, the peak is defined by fewer points, making an accurate fit to the correlation peak difficult to achieve, resulting in larger errors. When conducting sub-pixel interpolations small speckles have also been shown to result in phase errors and amplitude attenuation due to their high spectral content [14]. Similar results are expected from other DIC systems which use different methods of interpolation or curve fitting of the correlation function to achieve sub-pixel accuracy, as increasing the footprint of the correlation peak provides a greater number of points to inform any interpolation of the correlation function.

In practice it is highly impractical to create a speckle pattern with an optimised distribution, size and shape when applying the

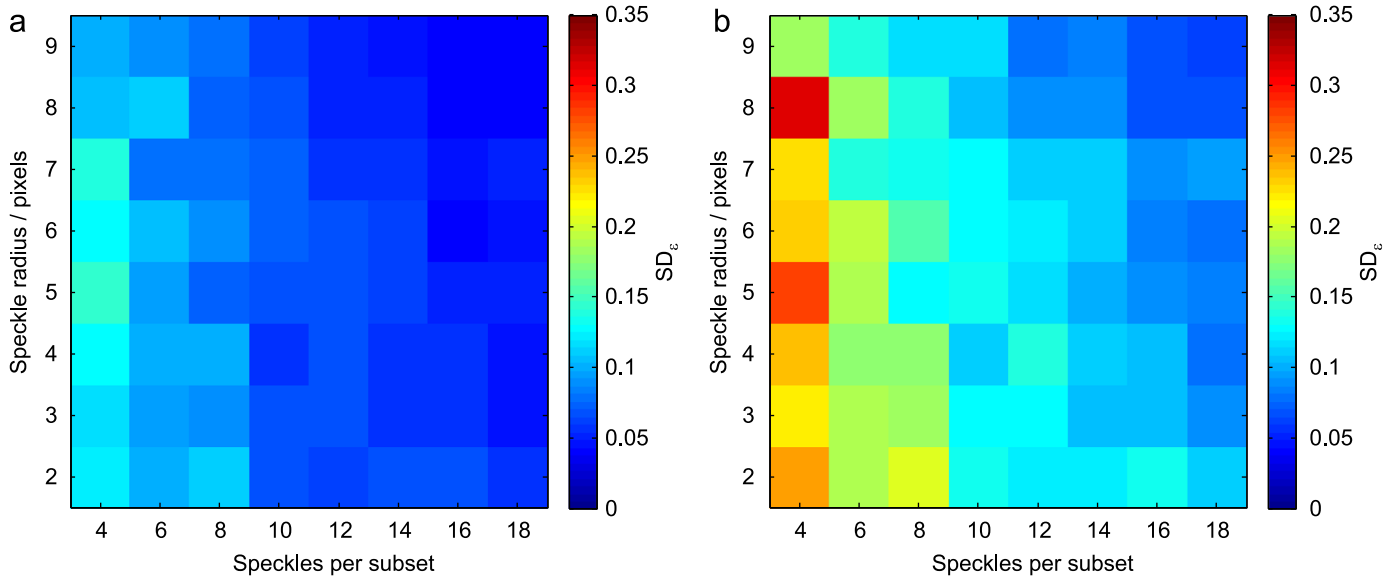

Fig. 2. (a) Error levels for speckle patterns at 1% strain and (b) 2% strain (Note: SD is in % strain).

pattern from an aerosol nozzle due to the random behaviour of the paint in the airflow. Therefore it is important that an informed speckle pattern assessment can be undertaken, building upon the general trends observed in this analysis.

4. Parameterised speckle pattern assessment

Pattern assessment has been previously discussed by a number of authors [10,15,16] offering a number of methods to evaluate the quality of the applied speckle pattern. Many of these methods have been focused on producing measures of pattern quality based upon the global properties of the pattern, and the information held within the image. It is important when considering the development of assessment criteria that it has sufficient technical knowledge supporting it. This was one of the main limitations identified by Pan et al. [9] on the morphological mean speckle size analysis conducted by Lecompte et al. [11]. Pan has presented a number of pattern quality criteria based upon the local subset intensity gradients [17] and the global mean intensity gradient throughout the image [9]. The latter showed good agreement to results obtained numerically, deforming the patterns at the sub-pixel level. The benefit of applying the global criteria is that they are straightforward to use. The limitation of the mean intensity gradient approach is that it does not give an indication of the randomness and uniqueness of the pattern locally from subset to subset. A simple means of global image assessment is to apply a parameter from information theory known as the Shannon entropy [18]; a measure of the information content of an image that is used for evaluating the randomness, or texture, of a form or pattern. An image with high entropy requires a large number of 'bits' to create an adequate representation of the form in a digital image. Hence a pattern with a high Shannon entropy value indicates a high level of texture, or broadness in the grey scale distribution of the image, both of which are beneficial for maximising the correlation function peak when a correct match has been found. The Shannon entropy is defined as [14]

$$\text{Shannon entropy} = \sum_{i=1}^{N} p(x_i)\log(p(x_i)) \tag{4}$$

where N is the grey level value and $p(x)$ is the count of pixels at the given grey level.

The Shannon entropy assessment measure was applied to the 64 generated images shown in Fig. 2. Fig. 4 shows a diagonal gradient of increasing Shannon entropy from bottom left to top right. This trend shows good agreement with the diagonal gradient of least measurement error observed in Fig. 2. The gradient in the Shannon entropy confirms the importance of the relationship between speckle size and shape, with larger, more uniquely defined speckles, which in turn provide more texture to the pattern so there is more spatial information in the image to benefit the correlation process. This analysis shows that the principal of the global measure works well with the controlled computer generated images.

The difficulty comes when applying this technique to patterns created in the laboratory by hand, where there is much less control over the size, shape and distribution of the pattern being applied. Table 1 shows the image entropy of 5 patterns created with black spray paint on a white background with similar grey level distributions at 5 different spatial resolutions from 23 to 705 pixels/mm. The different levels of magnification produce images with larger speckle sizes as magnification increases, replicating the variation in size of speckles in the patterns, as tested in the generated image analysis in Figs. 2 and 4.

There is little difference in the image entropy values between the patterns of markedly different spatial resolutions in Table 2, i.e. 23 and 705 pixels/mm and 37 and 296 pixels/mm give similar Shannon entropy values, although the patterns produced at these resolutions are vastly different in physical appearance. This illustrates how global pattern assessment criteria related to the image quality and information content can mask important local details of a pattern, which contribute significantly towards its suitability for use in as a DIC pattern. Unfortunately a complete assessment of the speckle pattern quality, taking into account differences due to the variation in the size or distribution of the speckles, cannot be made using the Shannon entropy. Therefore it is important to develop a methodology for pattern assessment based also upon local analysis of the pattern, which can determine changes in fundamental features of the stochastic pattern.

5. Morphological assessment of speckle characteristics

To provide a versatile tool to identify speckles within the images and the possibility of applying local assessment criteria

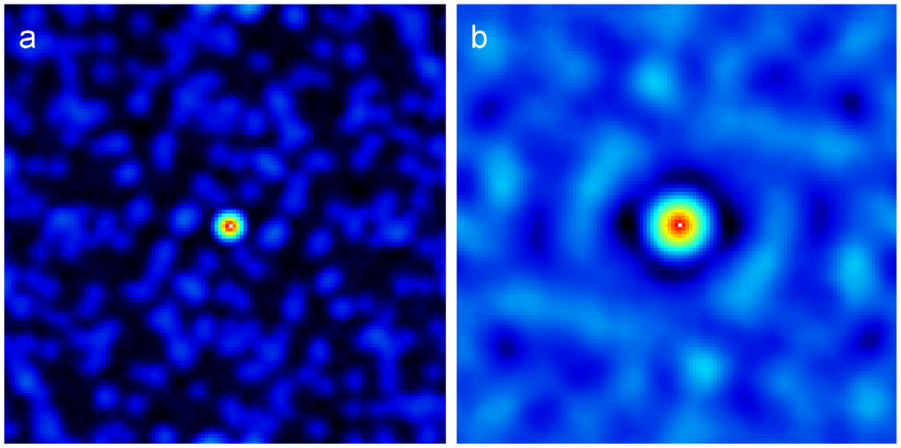

Fig. 3. Typical correlation function peak for pattern with speckle radius of (a) 3 pixels and (b) 8 pixels.

to the speckle pattern in the present work the Laplacian of Gaussian edge detection method is used to identify the individual speckles. Application of this method aims to remove the ambiguity of edge detection using the thresholding method by producing more accurate representations of the speckle size and shape. Firstly a Gaussian filter is applied to reduce noise from the image, and then the Laplacian operator is used to calculate the second spatial derivative of the image. From this, regions of rapid intensity change can be detected, that enables the identification of the edges of speckles. Accurate edge detection is controlled by careful adjustment of the Laplacian gradient value and standard deviation of the Gaussian filter. The process is shown in Fig. 5. In Fig. 5(a) a typical speckle pattern is shown and in Fig. 5(b) the edges detected by the Laplacian of Gaussian is shown. It can be seen in Fig. 5(b) that some edges are detected that do not form a closed contour around the speckle, so a 2D alpha shape technique is employed to reconstruct a closed contour from the pixels along the boundary. The alpha shape method formalises the intuitive notion of the 'shape' of a set of points. A generalisation of a 'convex hull' from the point set is created which describes the space enclosed by a set of points based on the outer most points [19]. The alpha shape generalisation to the convex hull allows concave as well as convex shapes to be mapped, creating a realistic border profile, better matching the actual shape of the pattern. From these closed contours a binary image of the speckle pattern is created for analysis as shown in Fig. 5(c).

Application of the edge detection method described above allows the size and number of the speckles to be analysed in any image. The edge detection methodology described above is applied to the same speckle patterns used for the image entropy analysis in Table 2, with spatial resolutions from 23 to 705 pixels/mm, which show inconsistent results. Fig. 6 shows the distributions of speckle sizes up to speckles with an area of 300 pixels in the pattern. The distribution of speckle sizes is expressed as a cumulative percentage of the total number of speckles in the pattern, identifying the frequency distribution of the speckle sizes present within the pattern. For example, a distribution with a straight diagonal line from 0%–100% would indicate an even distribution of speckle sizes within the pattern, such that each of the speckles in the pattern was a different size. Conversely, a distribution which showed a step change from 0% to 100% at the speckle size of 10 pixels would indicate that all the speckles within the pattern had a size of 10 pixels. The distributions have all been normalised by dividing by the coverage ratio of the pattern, (i.e. the total number of pixels defining the speckles divided by the total number of pixels in the image for each pattern). This removes any bias in the results caused by different speckle densities as opposed to morphometric

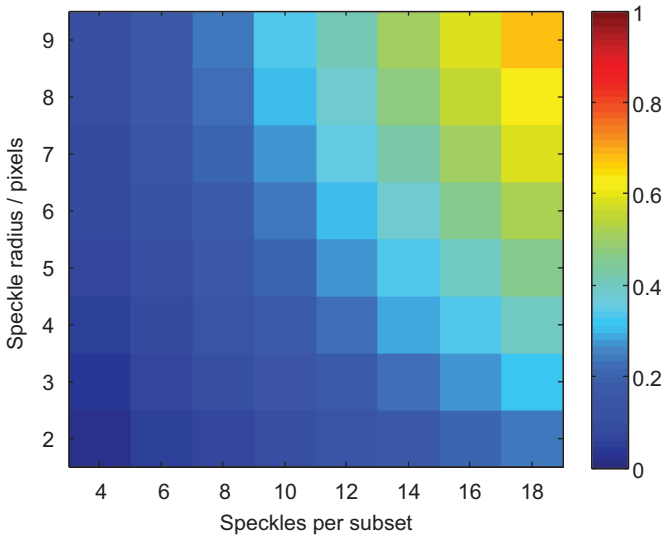

Fig. 4. Shannon image entropy.

differences due to the change in spatial resolution. From this the relative differences between the distributions of speckle sizes within the speckle patterns can be seen.

Fig. 6 shows clear differences between the fundamental components of the speckle patterns, which were not evaluated using the Shannon entropy measure of image information. Patterns identified as patterns containing similar information in Table 2 can now be seen to hold vastly different distributions of speckle sizes. At lower resolutions there are a very large proportion number of speckles with a size below 50 pixels, making up over 85% of the entire speckle in the pattern. As the spatial resolution of the image increases the gradient of the speckle size distribution decreases correspondingly, showing a more even distribution of speckle sizes within the pattern. This is due to better identification of small changes in the shape and size of the speckles at the higher spatial resolution, creating a more varied and random distribution of different shape and size speckles.

Although based on just 5 images, Fig. 6 clearly shows that the morphological edge detection technique can provide a much more informed view of the pattern properties compared to the Shannon entropy global image measure presented in Table 2. Clear differences between the patterns, not previously identifiable are now visible. The application of the technique produces an informed assessment of the properties of the pattern, providing a detailed method of comparative assessment of the physical differences

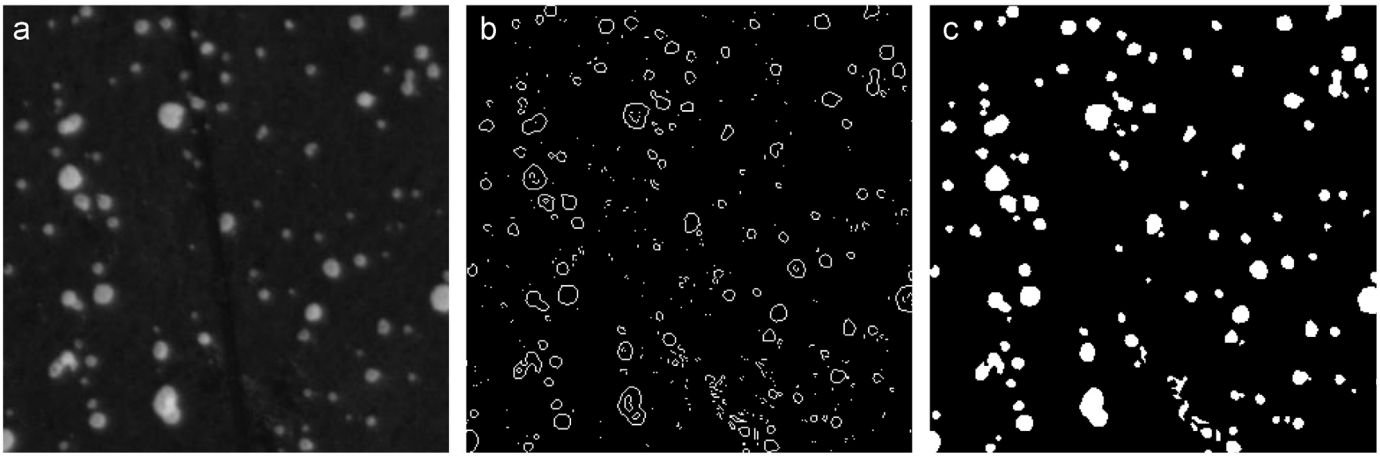

Fig. 5. (a) Speckle pattern image, (b) edge detection image and (c) binary speckle pattern.

between speckle patterns. This addresses the shortcomings of the global techniques and confirms the importance of conducting local analysis of the speckle pattern. The morphometric Laplacian of Gaussian and alpha shape reconstruction image processing parameters used in the methodology presented in this paper provide a large degree of control and flexibility to adapt to a wide range of speckle patterns, application methods and scales. This includes patterns where the grey level fluctuation provided by the painted speckle pattern is provided by the natural texture of the material, such as in the analysis of polymer bonded explosives [20] or the grain structure of metallics [21]. Natural patterns with a flat texture i.e. possessing very little contrast between features in the pattern, such as bare metallic surfaces [22,23] are less suitable for this methodology. However inconsistent illumination and reflections from these untreated surfaces are highly detrimental to the correlation so the application of a painted stochastic pattern is always strongly advised.

A detailed example of how this technique can be used to interpret these differences in pattern properties and optimise pattern selection to minimise measurement errors, increasing the confidence in the experimental results is discussed in the following sections.

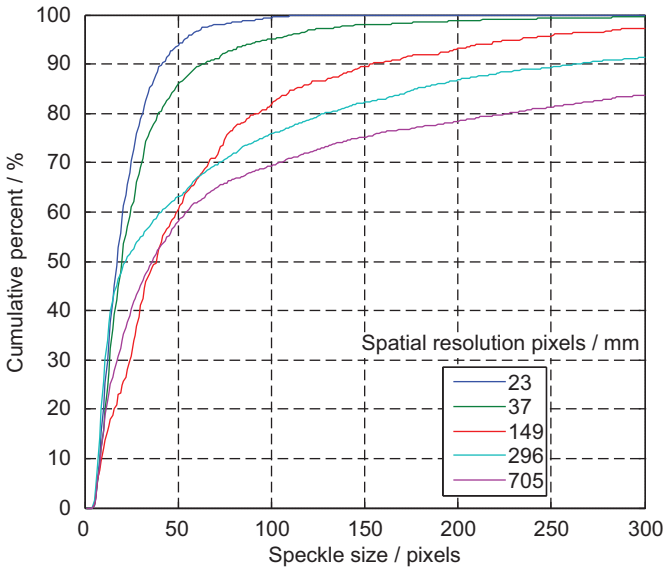

Fig. 6. Distribution of speckle sizes at varying levels of spatial resolution.

6. Application of morphological assessment to patterns with high image spatial resolutions

There are increasing numbers of white light imaging cameras available with large CCD arrays, delivering a high resolution images, with a large number of pixels/mm in the images. A high spatial resolution image allows large interrogation cells to be used, minimising the strain measurement uncertainty in the full field data, whilst maintaining a high spatial resolution of data points. Without high resolution imaging, smaller, less accurate interrogation cells have to be used to obtain a similar spatial resolution of analysed data points. A similar high resolution image result can be achieved with much cheaper, lower resolution cameras combined with the use of magnifying optics to achieve greater spatial resolution images over smaller regions of interest down to 3×3 mm [24–27]. Increasing magnification is usually used when strains are too small to be observed at lower resolutions, or when there are large, localised, gradients in the strain fields. When using magnifying optics, the observed shape, size and distribution of the applied speckle pattern is very different, to lower magnification images. This results in significantly different properties for the correlation algorithm to track. To achieve confidence in the repeatability and reproducibility of the measurements it is very important to ensure that the pattern is suitable for the optics in terms of size and shape of the speckles.

The morphological pattern assessment approach developed in the previous section was used to evaluate the difference between four pattern types, each with a different background colour and application method at high image resolution of 705 pixels/mm, identifying differences between them and equating those to pattern quality to minimise measurement errors. The patterns were painted on a flat plate of glass fibre epoxy composite material, which was sanded smooth to prevent the substrate texture influencing the quality of the applied patterns. To achieve a consistent pattern application methodology the paint was sprayed from a similar distance, with the same number of spray passes. Two different pattern application methods are investigated; spray paint and airbrush. A Clarke Wiz air compressor and airbrush kit was used to apply the airbrush patterns using Createx opaque paints for the speckles. High quality RS components matt black and white aerosols were used for the spray paint patterns. These two application methods were each tested with two different background colour combinations. A summary of the pattern application methods and magnification levels used is given in Table 3. Four samples of each pattern type were produced and analysed providing a sufficient sample for general trends between pattern application methods to be analysed. Examples of

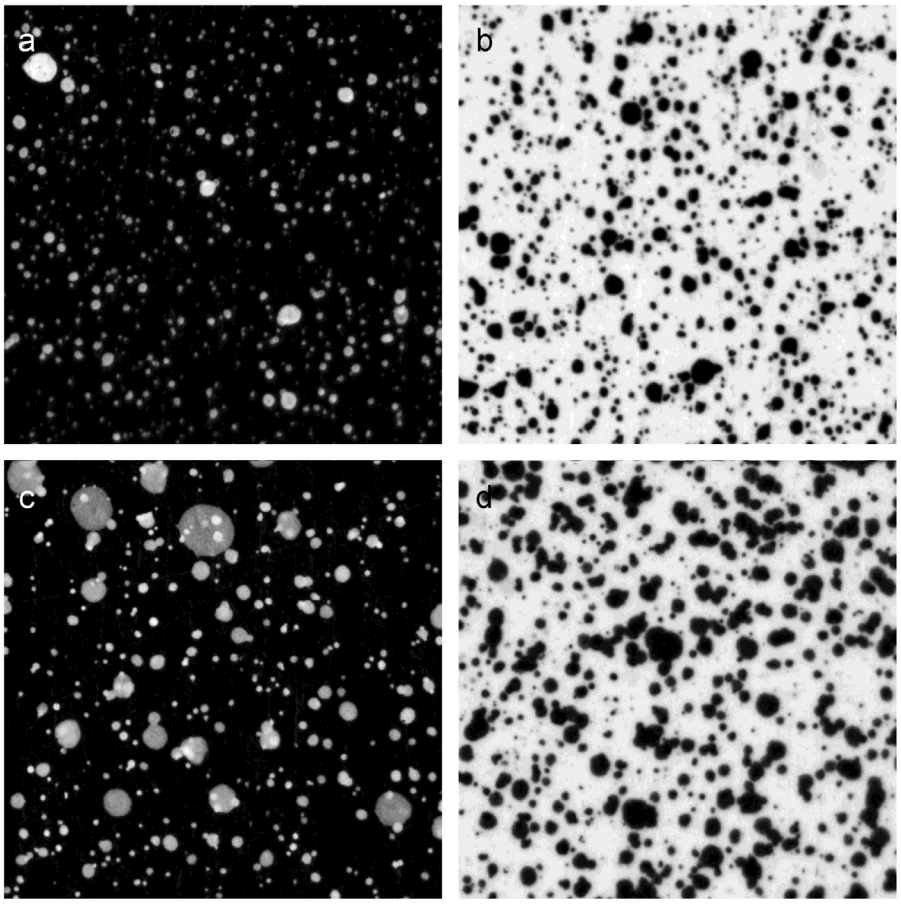

Fig. 7. Speckle patterns A–D used in the pattern assessment case study. (a) Pattern B (airbrush). (b) Pattern A (airbrush). (c) Pattern D (spray paint). (c) Pattern C (spray paint).

the patterns generated using the four methods defined in Table 2 are shown in Fig. 7.

Fig. 8 shows the mean distribution of speckle sizes from each of the four samples tested, for the four different pattern types as a cumulative percentage of the total coverage of the image. The distribution of the patterns can be seen to separate into two different distributions depending on application method. The distribution of spray paint patterns C, D have a steep gradient up to approximately 50 pixels, showing a high proportion, 60–80%, of speckles in the pattern below 50 pixels. Above 50 pixels the gradient decreases, showing a lower proportion of large speckles in the pattern. In contrast, the airbrush patterns show approximately 40–45% of speckles below 50 pixels, after which the gradient decreases and the proportion of speckles increases almost linearly with size up to 80% of the total speckles in the pattern. This indicates that the pattern possesses a more uniform distribution of speckle sizes greater than 50 pixels, within the pattern. The flatter gradient above 50 pixels also displays clearly how the airbrush produces an increased level of pattern uniqueness due to the larger size and hence increased shape and orientation permutations. In contrast, the distributions created by the spray paint are composed of predominantly small speckles which have less shape and orientation permutations within the pattern.

The analysis also shows that patterns with a white background, B and D, have a flatter distribution of speckle sizes than those with a black background A and C. This indicates fewer smaller speckles within the pattern. The difference in pattern distributions resulting from different background colours are much less than the differences created by changing the application method. The identification of fewer small speckles may be due to better

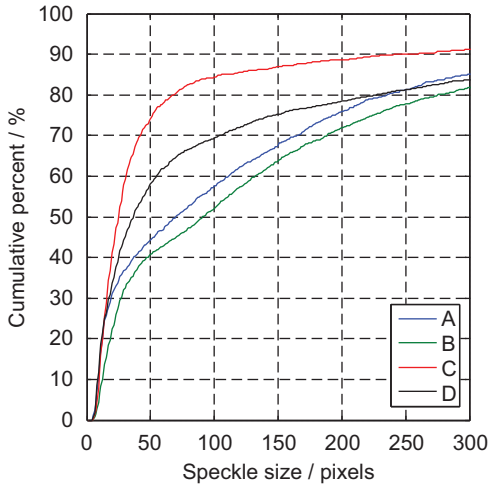

Fig. 8. Speckle size distribution—705 pixel/mm.

contrast of the black speckles on the white background and the narrower dynamic range of the background colour in the images, which possess less natural variation in background grey level compared to the white background.

Based upon the earlier analysis using the generated patterns, which saw higher errors for patterns possessing smaller speckles, it is concluded that the evenness of the distribution of speckle sizes in the higher resolution patterns will be beneficial to minimising the error in the DIC analysis. This suggests that the more even distribution of larger speckles for the Airbrush patterns, identified

from the morphological analysis, will correlate better than those made with spray paint. The broader, more even distribution, of speckle sizes above 50 pixels creates a pattern not only with a high uniqueness resulting from their size and shape. This is supported by the findings of the analysis of the simulated images, which identified the relationship between speckle size and coverage to the measurement error. It was that shown that larger speckle size patterns, which have greater shape uniqueness, provide lower measurement errors compared to subsets containing the same number of smaller sized speckles.

To test the hypothesis, that a broader distribution of speckle size measured by the morphological assessment method results in lower measurement error, a known displacement field was imposed on the images. The same image deformation technique as used in the earlier simulated pattern analysis was used. A linear *x*-direction displacement field was applied to give strain increments of 0.1% up to 1% maximum strain. The deformed images were imported into the correlation software Davis 7.4, and the error was assessed by calculating the standard deviation between the strain fields from the derived DIC result and the imposed deformation. The patterns were analysed using interrogation cell sizes of 128 × 128 pixels, with 0% overlap between subsets which is consistent with all of the previous analysed images in this paper.

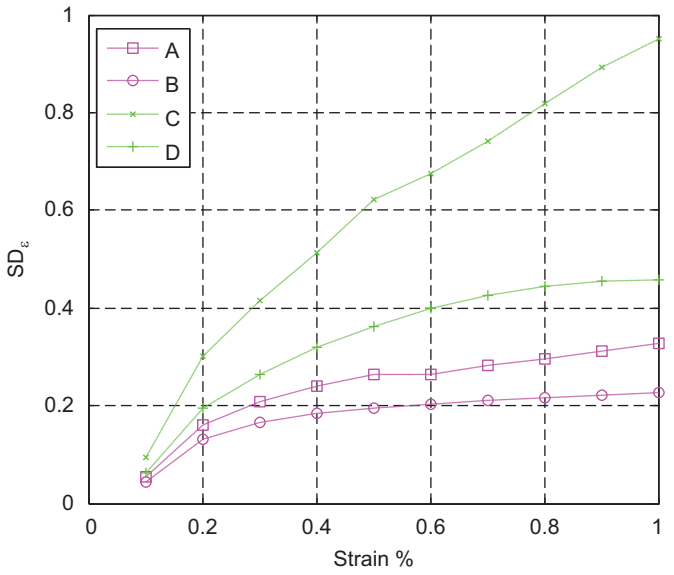

Fig. 9. Standard deviation of strain data at a 705 pixel/mm (Note: SD is in % strain).

Fig. 9 shows the mean SD error in strain for each of the four specimens tested for each pattern type. Very high standard deviation values are recorded for all patterns due to the sparseness of the patterns providing little grey level fluctuation to facilitate the correlation. This is shown in the clear distinction between the errors from the patterns created with an airbrush and spray paint. The airbrush patterns produce approximately half the error compared to those created with the spray paint, as its finer nozzle allows a more even coverage of speckles in the pattern, leaving less bare invariable background colour exposed within the subset. This shows good agreement with the predictions from the morphological analysis in Fig. 8, that more even distribution of speckle sizes in the airbrush patterns results in lower strain measurement errors. The spray paint patterns, which show a distribution of predominantly small speckles, appear to result in higher strain measurement error. These results also appear to support the findings of the initial numerical deformation study regarding the relationship between the speckle size, shape and error. The high error values illustrates the importance of examining the role of the speckle pattern in greater detail, showing that small changes in the pattern properties identified using the morphological approach yield large changes in the measured strain error. Fig. 7 shows that the background colour of the speckle pattern had little effect on changing the shape of the speckle pattern distributions for the airbrush patterns, with white backgrounds having slightly lower distribution curve gradients. Fig. 9 shows there to be little difference between the measurement errors for the two background colours for the airbrush, with the white background producing slightly lower error. However, for the spray painted specimens, the white background appears to produce almost half the error compared to patterns with a black background. This reflects the larger difference between the speckle distribution curves observed for pattern C and D in Fig. 8, compared with patterns A and B. This result also suggests that there is more natural variation in the grey level of the white background between the sparse speckles compared to in the black background, improving the correlation between images and lowering the contribution of the anomalous results on the standard deviation error measurement.

The results appear to show that analysis of the speckle pattern distribution using the morphological methodology is a good indicator of pattern quality. Validation of the morphological and

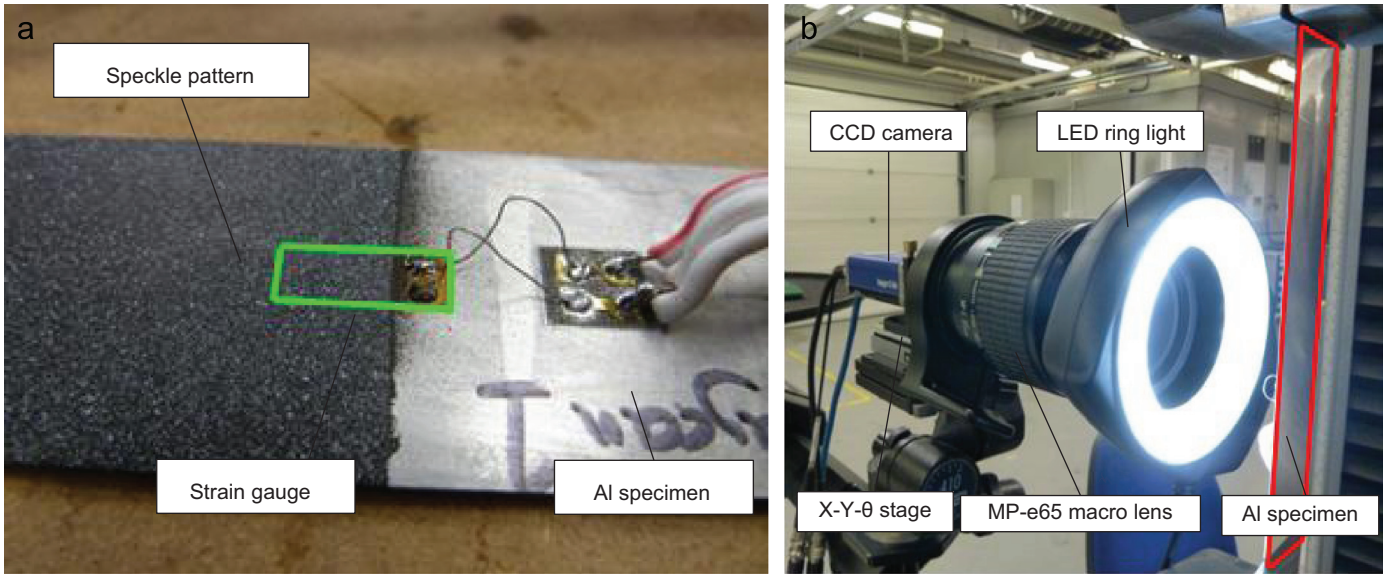

Fig. 10. (a) Detail view of strain gauge with speckle pattern applied on top and (b) experimental test setup.

numerical analysis was conducted by comparing experimental DIC and strain gauge results, evaluating the errors caused by the speckle pattern. 2D DIC was conducted on four 25 mm wide × 250 mm long × 1 mm thick rectangular aluminium specimens. Vishay CEA-06-240UZ-120 strain gauges with a 6 mm gauge length were bonded on to the surface of the specimens and a speckle pattern was applied over the surface of the specimen and strain gauge as shown in Fig. 10(a). Two specimens were painted using the airbrush and two with the spray paint. All specimens were painted with a black background with white speckles. Although it was shown above (see Fig. 9) that patterns with a white background produced less measurement error, the difference in error between the airbrush and spray paint is the largest for patterns with a black background. As such a black background is used to maximise the measurable difference in the DIC strain results between the patterns tested. The specimens were loaded in tension in an Instron servo-mechanical test machine up to 2 kN; giving an approximate applied strain of around 110 microstrain. Images were captured at 0.25 kN intervals using a 12 bit 5 Mp LaVision digital camera with image spatial resolutions very similar to the earlier analysis of 712 pixels/mm. The camera was mounted on an X–Y–θ stage, to allow fine adjustment of the focal plane. This ensured as practically as possible that the camera was parallel to the specimen surface during the test, minimising errors from misalignment of the optical setup. Some out-of-plane displacement is inevitable in this set-up however but it was not possible to conduct 3D DIC using the microscope stage due to the lens size and short focal distance. The experimental setup is shown in Fig. 10(b). DIC was performed using the LaVision DaVis 7.4 software, with the area of interest directly over the strain gauge, once again using 128 × 128 subset sizes to remain consistent in the analysis of the patterns conducted in this paper. The data from the strain gauge were compared to the average of the DIC data from the interrogation cells covering the strain gauge.

Fig. 11 shows a comparison between the mean strain measurements recorded using the strain gauge and the DIC for the two specimens tested for each paint application method. The DIC strain data for the airbrush pattern and the strain gauge match very well, with a slight oscillation in the strain measurement. In contrast there is a large difference between the results from the DIC using the spray paint pattern and the strain gauge data, with the DIC producing consistently lower strain measurements. This result confirms the numerical deformation analysis and the use of the morphological assessment of the speckle size distribution which had both identified the airbrush pattern as producing the least measurement error due to the more even distribution of speckle sizes within the pattern. This also validates the analysis of the speckle pattern distribution using the morphological method as a good initial identifier of pattern quality. From the pattern assessment methodology it has been shown that the distribution of larger speckles appears to have a beneficial effect, providing patterns with a high degree of uniqueness between the speckles in the pattern, and also producing patterns which are more resistant to the uncertainties in speckle location created from of image noise. In this case, as shown in Fig. 9, the best quality pattern, delivering the least measurement error is created using a black pattern on a white background produced from an airbrush.

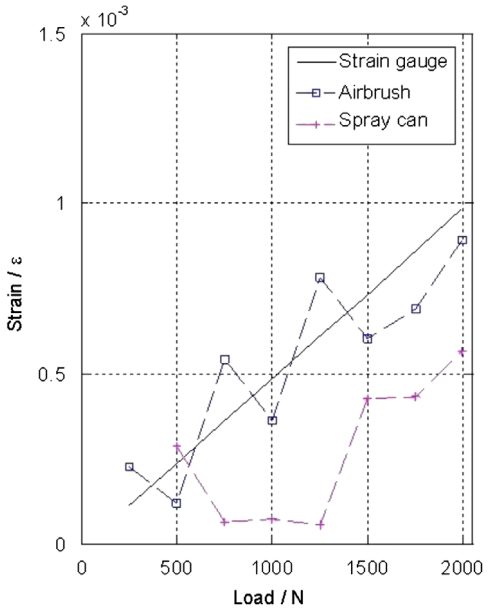

Fig. 11. Strain gauge/DIC comparison at 712 pixel/mm.

7. Conclusions

The work described in the paper has demonstrated the use of image processing techniques to evaluate the effect of physical changes of speckle patterns on image correlation. An evaluation of the effect of speckle size and coverage in speckle patterns was conducted using numerically deformed images, which identified a clear relationship between the measurement error and the uniqueness of a pattern resulting from the speckle size and shape. Errors reduced with increasing number of speckles in the pattern, with larger sized speckles providing a greater variation of shape, resulting in a lower error than patterns with smaller speckles.

Global pattern quality parameters were discussed and Shannon entropy was used as an example to demonstrate that the global measures are not sufficient to assess the quality and properties of the pattern. This was illustrated by comparing patterns with vastly different spatial resolutions. As a result a morphological approach is presented using the Laplacian of Gaussian edge detection method, successfully identifying the edges of speckles and overcoming some of the shortfalls of image thresholding techniques. This method was compared against the Shannon entropy measure and identified large changes to the distribution of the speckle sizes with increasing spatial resolution of image which could not be established with using the image entropy assessment.

A detailed example of the morphological assessment methodology was presented using patterns with high spatial resolution as the test case, which are typically used when using high magnification DIC, where the strains are often small and measurement precision is very important. Clear links were identified between the levels of measurement error due to the pattern and the evenness of the speckle size distribution in the applied speckle pattern. Numerical deformation and experimental comparison of 2D DIC against strain gauge readings was used to validate this assessment approach, identifying patterns which showed the most even distribution of speckle sizes in the morphological assessment to result in the lowest errors. Systematic errors resulting from the correlation algorithm used in the software were not assessed.

Acknowledgements

The work described in this paper is supported by the UK Engineering and Physical Sciences Research Council and by a Stanley Grey Fellowship awarded by the Institute of Marine Engineering, Science & Technology.

References

[1] Triconnet K, Derrien K, Hild F, Baptiste D. Parameter choice for optimized digital image correlation. Opt Lasers Eng 2009;47(6):728–37.

[2] Yaofeng S, Pang J. Study of optimal subset size in digital image correlation of speckle pattern images. Opt Lasers Eng 2007;45(9):967–74.

[3] Schreier HW, Sutton MA. Systematic errors in digital image correlation due to undermatched subset shape functions. Exp Mech 2002;42(3):303–10.

[4] Schreier HW, Braasch JR, Sutton MA. Systematic errors in digital image correlation caused by intensity interpolation. Opt Eng 2000;39(11):2915.

[5] Hung P-C, Voloshin AS. In-plane strain measurement by digital image correlation. J Braz Soc Mech Sci Eng 2003;25(3).

[6] Haddadi H, Belhabib S. Use of rigid-body motion for the investigation and estimation of the measurement errors related to digital image correlation technique. Opt Lasers Eng 2008;46(2):185–96.

[7] Barranger Y, Doumalin P, Dupré JC, Germaneau A. Digital image correlation accuracy: influence of kind of speckle and recording setup. EPJ Web Conf 2010;6:31002.

[8] Pan B, Xie H, Wang Z, Qian K, Wang Z. Study on subset size selection in digital image correlation for speckle patterns. Opt Express 2008;16(10):7037–48.

[9] Pan B, Lu Z, Xie H. Mean intensity gradient: an effective global parameter for quality assessment of the speckle patterns used in digital image correlation. Opt Lasers Eng 2010;48(4):469–77.

[10] Hua T, Xie H, Wang S, Hu Z, Chen P, Zhang Q. Evaluation of the quality of a speckle pattern in the digital image correlation method by mean subset fluctuation. Opt Lasers Eng 2011;43(1):9–13.

[11] Lecompte D, Smits A, Bossuyt S, Sol H, Vantomme J, Van Hemelrijck D, et al. Quality assessment of speckle patterns for digital image correlation. Opt Lasers Eng 2006;44(11):1132–45.

[12] Alexander TL, Harvey JE, Weeks AR. Average speckle size as a function of intensity threshold level: comparison of experimental measurements with theory. Appl Opt 1994;33(35).

[13] Pan B, Qian K, Xie H, Asundi A. Two-dimensional digital image correlation for in-plane displacement and strain measurement: a review. Meas Sci Technol 2009;20(6):062001.

[14] Lecompte D, Bossuyt S, Cooreman S, Sol H, Vantomme J. Study and generation of optimal speckle patterns for DIC. In: Proceedings of the SEM annual conference and exposition on experimental and applied mechanics; 2007.

[15] Sutton MA, Orteu J-J, Schreier HW. Image correlation for shape, motion and deformation measurements: basic concepts. Theory Appl 2009, ISBN 978-0-387-78747-3.

[16] Lane C, Burguete RL, Shterenlikht A. An objective criterion for the selection of an optimum DIC pattern and subset size. In: Proceedings of the SEM XI international congress and exposition on experimental and applied mechanics; 2008.

[17] Pan B, Xie H, Wang Z, Qian K, Wang Z. Study on subset size selection in digital image correlation for speckle patterns. Opt Express 2008;16(10):7037.

[18] Shannon C. A mathematical theory of communication. Bell Syst Techn J 1948;27:379.

[19] Edelsbrunner H, Kirkpatrick DG, Seidel R. On the shape of a set of points in the plane. IEEE Trans Inf Theory 1983;29(4):551. http://dx.doi.org/10.1109/TIT.1983.1056714.

[20] Rae P, Palmer SJ, Goldrein H, Lewis A, Field J. White-light digital image cross-correlation (DICC) analysis of the deformation of composite materials with random microstructure. Opt Lasers Eng 2004;41(4):635–48.

[21] El Bartali A, Aubin V, Degallaix S. Fatigue damage analysis in a duplex stainless steel by digital image correlation technique. Fatigue Fract Eng Mater Struct 2008;31(2):137–51.

[22] Zhang D, Arola D, Luo M. Characterization of mechanical properties on the meso-scale with digital image correlation. In: Proceedings of the SEM X international congress and exposition on experimental and applied mechanics; 2004.

[23] Zhang D, Luo M, Arola DD. Displacement/strain measurements using an optical microscope and digital image correlation. Opt Eng 2006;45(3):033605.

[24] Kirugulige MS, Tippur HV, Denney TS. Measurement of transient deformations using digital image correlation method and high-speed photography: application to dynamic fracture. Appl Opt 2007;46(22):5083–96.

[25] Gao J, Shang H. Deformation-pattern-based digital image correlation method and its application to residual stress measurement. Appl Opt 2009;48(7):1371.

[26] Lord JD, Penn D, Whitehead P. The application of digital image correlation for measuring residual stress by incremental hole drilling. Appl Mech Mater 2008;13–14:65–73.

[27] Poncelet M, Barbier G, Raka B, Courtin S, Desmorat R, Le-Roux JC, et al. DIC-aided biaxial fatigue tests of a 304L steel. EPJ Web Conf 2010;6:16002.